

Contents lists available at ScienceDirect

Journal of Sound and Vibration

journal homepage: www.elsevier.com/locate/jsvi



On the use of a Prandtl-Glauert-Lorentz transformation for acoustic scattering by rigid bodies with a uniform flow



Fang Q. Hu^{a,*}, Michelle E. Pizzo^a, Douglas M. Nark^b

- ^a Department of Mathematics and Statistics, Old Dominion University, Norfolk, VA 23529, USA
- ^b Structural Acoustics Branch, NASA Langley Research Center, Hampton, VA 23681, USA

ARTICLE INFO

Article history: Received 23 December 2017 Revised 28 September 2018 Accepted 26 November 2018 Available online 27 November 2018 Handling Editor: J. Astley

Keywords: Acoustic scattering Boundary condition Mean flow effects Space-time transformation

ABSTRACT

It is well-known that the convective wave equation with a uniform mean flow can be transformed into a standard wave equation without flow by a Prandtl-Glauert-Lorentz type transformation. This paper examines the boundary condition to be used in the transformed coordinates for acoustic scattering by rigid bodies. Recently, based on the energy conservation equation for acoustic waves propagating in a uniform flow, a new solid wall boundary condition, dubbed the Zero Energy Flux (ZEF) solid surface boundary condition, has been proposed. Instead of the commonly used solid surface boundary condition that the normal acoustic velocity be zero, the ZEF condition requires that the acoustic energy flux be zero. In this paper, we point out that when formulated in the acoustic velocity potential and under the ZEF boundary condition, the normal derivative of the velocity potential remains to be zero when computed in the transformed coordinates. As such, numerical methods developed for solving the standard wave equation can be directly applied to the convective wave equation through a use of the Prandtl-Glauert-Lorentz transformation. Utilization of the transformation is particularly beneficial for numerical methods based on the boundary integral formulation because of the simplified kernel function in the transformed coordinates, for both the time domain and the frequency domain approaches. Useful relations for applying the transformation are derived and numerical examples that demonstrate the effectiveness of the transformation and ZEF boundary condition are presented.

© 2018 Elsevier Ltd. All rights reserved.

1. Introduction

Under the assumption of a uniform mean flow, acoustic wave propagation is governed by the convective wave equation [21]. It has long been known that the convective wave equation can be transformed into the standard wave equation without flow by using a Prandtl-Glauert type transformation [1,2,4,6,8,9,12,16,18,23,24,27]. The Prandtl-Glauert transformation was originally made to study the effect of compressibility on the lift of an airfoil where the linearized static velocity potential equation was transformed into one of incompressible flows [9]. Extension of the Prandtl-Glauert transformation to time-dependent aerodynamic problems has been made in Refs. [1,16,18,24], which consisted mainly of a combination of Galilean transformation and Lorentz transformation. For aeroacoustic applications, similar transformations were proposed by Taylor [27] for the study of wind-tunnel flow effects on sound propagation where the mean flow condition was extended to include steady homeotropic potential flows at low Mach numbers. In Ref. [7], similarity variables were developed for sound radiation in uniform flows

E-mail address: fhu@odu.edu (F.Q. Hu).

^{*} Corresponding author.

based on the so-called Prandtl-Glauert coordinates. In a different approach, a space-time Lorentz transformation was studied for aeroacoustic problems using Geometric Algebra in Ref. [10]. Use of such transformations in boundary element methodology was first presented in Ref. [2] for acoustic radiation and scattering by applying Taylor's transformation to the acoustic perturbation equation for low Mach number flows. More recently, an assessment of the Taylor-Lorentz transformation for the boundary element method was given in Ref. [17], and an application of the Lorentz transformation to the equivalence source method in the frequency domain was presented in Ref. [28]. For these historical developments, the transformation with uniform mean flows discussed in this paper will be referred to as Prandtl-Glauert-Lorentz transformation.

This paper is concerned with the boundary condition to be applied at solid surfaces under the Prandtl-Glauert-Lorentz transformation. While the aforementioned transformations can be used to reduce the convective wave equation into the standard wave equation, one potential concern has been that the use of the transformation "does not lead to a much simpler boundary-value problem in the transformed space" when physical boundaries are present [1]. This is understandable, because the boundaries are necessarily deformed under the transformation and, consequently, the boundary condition is also expected to be modified. Consider the usual solid wall boundary condition for acoustic waves which states that the normal velocity, or the normal derivative of the velocity potential, becomes zero at solid surfaces. As body surfaces are deformed by the transformation, the surface normal vectors will obviously no longer be the same in the two coordinates, and, as we will show later, application of the usual solid wall boundary condition would indeed lead to a more complicated normal derivative in transformed coordinates.

Recently, based on the acoustic energy conservation equation, an alternative solid wall boundary condition has been proposed for computing acoustic wave scattering in the presence of a uniform flow [14]. Unlike the commonly applied boundary condition that the normal velocity of the acoustic wave be zero, the new boundary condition instead requires that the acoustic energy flux be zero at solid surfaces. The new boundary condition was referred to in Ref. [14] as the Zero Energy Flux (ZEF) condition. In this paper, we show that an application of the ZEF solid wall boundary condition preserves the usual solid wall boundary condition of no flow under the Prandtl-Glauert-Lorentz transformation. The simplicity of the boundary condition in the transformed domain should render the Prandtl-Glauert-Lorentz transformation an attractive tool for finding numerical solutions for scattering by rigid bodies in the presence of flow.

The rest of the paper is organized as follows: A detailed derivation of the generalized Prandtl-Glauert-Lorentz transformation is presented in Section 2. In Section 3, the solid wall boundary condition to be applied in the transformed coordinates is discussed and derived. Section 4 works out some useful relations between the solutions in the transformed and the original physical space-time coordinates. Numerical examples of wave scattering by a solid body are presented in Section 5 that demonstrate the utility of the Prandtl-Glauert-Lorentz transformation. Section 6 contains the conclusions.

2. Generalized Prandtl-Glauert-Lorentz transformation

In this section, we first present a derivation of the generalized Prandtl-Glauert-Lorentz space-time transformation for mean flows in a general direction. In the literature, the transformations are often given for the special case where the mean flow coincides with one of the spatial axes. The current derivation is presented from the point view of transforming the partial differential equation. The properties of the transformation discussed in this section will also become useful for deriving the solid wall boundary condition in the next section.

Consider the convective wave equation written as

$$\left(\frac{\partial}{\partial t} + \mathbf{U} \cdot \nabla\right)^2 \phi - c^2 \nabla^2 \phi = q(x, y, z, t),\tag{1}$$

where c is the speed of sound, q(x, y, z, t) is a source term, and \boldsymbol{U} is the uniform mean velocity vector defined as

$$\mathbf{U} = \begin{bmatrix} U_1 \\ U_2 \\ U_3 \end{bmatrix}. \tag{2}$$

Here, $\phi(x, y, z, t)$ is the acoustic velocity potential where the acoustic pressure p and acoustic velocity u are related to ϕ as follows:

$$p(x, y, z, t) = -\rho_0 \left(\frac{\partial \phi}{\partial t} + \mathbf{U} \cdot \nabla \phi \right), \quad \mathbf{u} = \nabla \phi, \tag{3}$$

where ρ_0 is the mean density. In this study, solution of Eq. (1) is considered in the context of scattering of acoustic waves by rigid bodies bounded by a surface, or a collection of surfaces, *S*.

We look for a linear space-time transformation of the following form,

$$t' = a_0 t + b_1 x + b_2 y + b_3 z,$$

$$x' = a_{11} x + a_{12} y + a_{13} z,$$

$$y' = a_{21} x + a_{22} y + a_{23} z,$$

$$z' = a_{31} x + a_{32} y + a_{33} z,$$
(4)

such that Eq. (1) is transformed to the standard wave equation without flow in space coordinates (x', y', z') and time t'. Note that, in the above, the transformation in space is taken to be independent of time. In this way, spatial boundaries in the transformed domain will remain stationary and independent of time. For convenience of discussion, we denote

$$\mathbf{A} = \begin{bmatrix} a_{11} & a_{12} & a_{13} \\ a_{21} & a_{22} & a_{23} \\ a_{31} & a_{32} & a_{33} \end{bmatrix} \text{ and } \mathbf{b} = \begin{bmatrix} b_1 \\ b_2 \\ b_3 \end{bmatrix}.$$
 (5)

Then, transformation for the spatial derivatives can be found as follows:

$$\begin{bmatrix} \frac{\partial}{\partial x} \\ \frac{\partial}{\partial y} \\ \frac{\partial}{\partial z} \end{bmatrix} = \begin{bmatrix} b_1 & a_{11} & a_{21} & a_{31} \\ b_2 & a_{12} & a_{22} & a_{32} \\ b_3 & a_{13} & a_{23} & a_{33} \end{bmatrix} \begin{bmatrix} \frac{\partial}{\partial t'} \\ \frac{\partial}{\partial x'} \\ \frac{\partial}{\partial y'} \\ \frac{\partial}{\partial z'} \end{bmatrix} = \begin{bmatrix} \mathbf{b} & \mathbf{A}^T \end{bmatrix} \begin{bmatrix} \frac{\partial}{\partial t'} \\ \frac{\partial}{\partial x'} \\ \frac{\partial}{\partial y'} \\ \frac{\partial}{\partial z'} \end{bmatrix}. \tag{6}$$

A superscript T denotes the transpose of the matrix. Using Eq. (6), it is straight forward to find that the convective wave Eq. (1) becomes the following in the transformed coordinates:

$$\begin{bmatrix} \frac{\partial}{\partial t'} \\ \frac{\partial}{\partial \lambda'} \\ \frac{\partial}{\partial y'} \\ \frac{\partial}{\partial z'} \end{bmatrix}^{T} \begin{pmatrix} \left[(a_{0} + \mathbf{U}^{T} \mathbf{b})^{2} & (a_{0} + \mathbf{U}^{T} \mathbf{b}) \mathbf{U}^{T} \mathbf{A}^{T} \\ (a_{0} + \mathbf{U}^{T} \mathbf{b}) \mathbf{A} \mathbf{U} & \mathbf{A} \mathbf{U} \mathbf{U}^{T} \mathbf{A}^{T} \end{bmatrix} - c^{2} \begin{bmatrix} \mathbf{b}^{T} \mathbf{b} & \mathbf{b}^{T} \mathbf{A}^{T} \\ \mathbf{A} \mathbf{b} & \mathbf{A} \mathbf{A}^{T} \end{bmatrix} \right) \begin{bmatrix} \frac{\partial \phi}{\partial t'} \\ \frac{\partial \phi}{\partial x'} \\ \frac{\partial \phi}{\partial y'} \\ \frac{\partial \phi}{\partial z'} \end{bmatrix} = q.$$
 (7)

We wish to determine the transformation such that the above is the standard wave equation, namely, we wish to choose a_0 , b, and A in Eq. (4) such that

$$\begin{bmatrix} (a_0 + \mathbf{U}^T \mathbf{b})^2 & (a_0 + \mathbf{U}^T \mathbf{b}) \mathbf{U}^T \mathbf{A}^T \\ (a_0 + \mathbf{U}^T \mathbf{b}) \mathbf{A} \mathbf{U} & \mathbf{A} \mathbf{U} \mathbf{U}^T \mathbf{A}^T \end{bmatrix} - c^2 \begin{bmatrix} \mathbf{b}^T \mathbf{b} & \mathbf{b}^T \mathbf{A}^T \\ \mathbf{A} \mathbf{b} & \mathbf{A} \mathbf{A}^T \end{bmatrix} = \begin{bmatrix} 1 & 0 & 0 & 0 \\ 0 & -c^2 & 0 & 0 \\ 0 & 0 & -c^2 & 0 \\ 0 & 0 & 0 & -c^2 \end{bmatrix}.$$
 (8)

This leads to the following requirements for the transformation defined in Eq. (4):

$$\left(a_0 + \mathbf{U}^T \mathbf{b}\right)^2 - c^2 \mathbf{b}^T \mathbf{b} = 1,\tag{9}$$

$$\left[\left(a_0 + \mathbf{U}^T \mathbf{b} \right) \mathbf{U}^T - c^2 \mathbf{b}^T \right] \mathbf{A}^T = \mathbf{0}, \tag{10}$$

$$\mathbf{A}\mathbf{U}\mathbf{U}^{T}\mathbf{A}^{T} - c^{2}\mathbf{A}\mathbf{A}^{T} = -c^{2}\mathbf{I}. \tag{11}$$

Solving Eqs. (9) and (10) simultaneously for a_0 and b, we get the following unique solution:

$$a_0 = \alpha, \quad \mathbf{b} = \frac{\mathbf{M}}{\alpha c},$$
 (12)

where

$$\alpha = \sqrt{1 - M^2}, \quad \mathbf{M} = \mathbf{U}/c = \begin{bmatrix} M_1 \\ M_2 \\ M_3 \end{bmatrix}, \quad M = |\mathbf{M}| = \sqrt{M_1^2 + M_2^2 + M_3^2}.$$
 (13)

The solution of Eq. (11) for \boldsymbol{A} however would not be unique. One solution is that found in the Lorentz transformation in the theory of special relativity [15,28]. For a general velocity vector \boldsymbol{M} , the solution for \boldsymbol{A} in Eq. (11) is

$$\mathbf{A} = \mathbf{I} + \frac{1}{\alpha(1+\alpha)} \mathbf{M} \mathbf{M}^{T} = \mathbf{I} + \frac{1}{\alpha(1+\alpha)} \begin{bmatrix} M_{1}^{2} & M_{1}M_{2} & M_{1}M_{3} \\ M_{1}M_{2} & M_{2}^{2} & M_{2}M_{3} \\ M_{1}M_{3} & M_{2}M_{3} & M_{3}^{2} \end{bmatrix},$$
(14)

where *I* is the identity matrix.

Hence, the space-time transformation (4) that we sought for stated explicitly is:

$$t' = \alpha t + \frac{1}{\alpha c} \left(M_1 x + M_2 y + M_3 z \right),$$

$$x' = x + \frac{M_1}{\alpha (1 + \alpha)} \left(M_1 x + M_2 y + M_3 z \right),$$

$$y' = y + \frac{M_2}{\alpha (1 + \alpha)} \left(M_1 x + M_2 y + M_3 z \right),$$

$$z' = z + \frac{M_3}{\alpha (1 + \alpha)} \left(M_1 x + M_2 y + M_3 z \right),$$
(15)

or, in vector notation,

$$t' = \alpha t + \frac{1}{\alpha c} (\mathbf{M} \cdot \mathbf{r}), \quad \mathbf{r}' = \mathbf{A}\mathbf{r} = \mathbf{r} + \frac{(\mathbf{M} \cdot \mathbf{r})}{\alpha (1 + \alpha)} \mathbf{M}, \tag{16}$$

where

$$\mathbf{r} \equiv \begin{bmatrix} x \\ y \\ z \end{bmatrix}, \quad \mathbf{r}' \equiv \begin{bmatrix} x' \\ y' \\ z' \end{bmatrix}. \tag{17}$$

Under such a transformation, the convective wave Eq. (1) becomes the following standard wave equation without flow:

$$\frac{\partial^2 \Phi}{\partial t'^2} - c^2 \nabla'^2 \Phi = Q(x', y', z', t'),\tag{18}$$

where $\Phi(x', y', z', t') = \phi(x, y, z, t)$ and Q(x', y', z', t') = q(x, y, z, t) denote, respectively, the solution and source term in transformed coordinates.

It is also easy to find the inverse for transformation (15), as we have conveniently

$$\mathbf{A}^{-1} = \mathbf{I} - \frac{1}{1+\alpha} \mathbf{M} \mathbf{M}^{T} = \mathbf{I} - \frac{1}{1+\alpha} \begin{bmatrix} M_{1}^{2} & M_{1} M_{2} & M_{1} M_{3} \\ M_{1} M_{2} & M_{2}^{2} & M_{2} M_{3} \\ M_{1} M_{3} & M_{2} M_{3} & M_{3}^{2} \end{bmatrix}.$$
(19)

We note that both \mathbf{A} and \mathbf{A}^{-1} are symmetric matrices. In addition, it can be shown that the following properties are true:

$$\mathbf{A}\mathbf{M} = \frac{1}{\alpha}\mathbf{M}, \quad \mathbf{A}^{-1}\mathbf{M} = \alpha\mathbf{M},\tag{20}$$

and

$$\mathbf{A}\mathbf{A}^{T} = \frac{1}{\alpha^{2}}\mathbf{M}\mathbf{M}^{T} + \mathbf{I}, \quad \mathbf{A}^{-1}\left[\mathbf{A}^{-1}\right]^{T} = -\mathbf{M}\mathbf{M}^{T} + \mathbf{I}.$$
 (21)

Finally, the inverse transformation for Eq. (15) can be written as follows:

$$t = \frac{1}{\alpha}t' - \frac{1}{\alpha c}\left(\mathbf{M} \cdot \mathbf{r}'\right), \quad \mathbf{r} = \mathbf{A}^{-1}\mathbf{r}' = \mathbf{r}' - \frac{\left(\mathbf{M} \cdot \mathbf{r}'\right)}{1 + \alpha}\mathbf{M}.$$
 (22)

We note that the space-time transformation (15) is not exactly the same as the Lorentz transformation in the theory of special relativity, which would be a transformation between \mathbf{r}' and a moving frame \mathbf{r}'' where $\mathbf{r}'' = \mathbf{r} - \mathbf{U}t$.

3. Boundary condition at solid surfaces

We now consider the problem of scattering by solid surfaces and study a suitable boundary condition to be used in the transformed coordinates. A commonly applied solid wall boundary condition has been that the normal velocity of the acoustic wave, or the normal derivative of the velocity potential ϕ , be zero. Now as body surfaces are deformed by the space-time transformation (15), the surface normal vectors will obviously no longer be the same in the two coordinates. Suppose a surface defined by equation f(x, y, z) = 0 in space (x, y, z) is transformed to be F(x', y', z') = 0 in the (x', y', z') coordinates. Then, by Eq. (6), we have the following relation for their normal directions:

$$\nabla' F = \begin{bmatrix} \frac{\partial F}{\partial x'} \\ \frac{\partial F}{\partial y'} \\ \frac{\partial F}{\partial z'} \end{bmatrix} = \begin{bmatrix} \mathbf{A}^{-1} \end{bmatrix}^T \begin{bmatrix} \frac{\partial f}{\partial x} \\ \frac{\partial f}{\partial y} \\ \frac{\partial f}{\partial z} \end{bmatrix} = \begin{bmatrix} \mathbf{A}^{-1} \end{bmatrix}^T \nabla f. \tag{23}$$

Let n and n' be respectively the unit normal vectors of the scattering surface in space coordinates (x, y, z) and (x', y', z'). Then, we have

$$\mathbf{n}' = \frac{\nabla' F}{|\nabla' F|} = \frac{\left[\mathbf{A}^{-1}\right]^T \nabla f}{\left|\left[\mathbf{A}^{-1}\right]^T \nabla f\right|} = \frac{|\nabla f|}{\left|\left[\mathbf{A}^{-1}\right]^T \nabla f\right|} \left[\mathbf{A}^{-1}\right]^T \mathbf{n} \equiv \mu \left[\mathbf{A}^{-1}\right]^T \mathbf{n},\tag{24}$$

where μ is a scalar factor such that \mathbf{n}' is a unit vector.

On the other hand, for the normal derivative of the solution $\Phi(x', y', z', t')$ in the transformed coordinates, by using relations (20) and (21), we have

$$\frac{\partial \Phi}{\partial n'} = \mathbf{n}' \cdot \nabla' \Phi = \mathbf{n}'^T \begin{bmatrix} \frac{\partial \Phi}{\partial x'} \\ \frac{\partial \Phi}{\partial y'} \\ \frac{\partial \Phi}{\partial z'} \end{bmatrix} = \mu \mathbf{n}^T \mathbf{A}^{-1} \begin{pmatrix} -\frac{1}{\alpha c} \frac{\partial \phi}{\partial t} \mathbf{M} + [\mathbf{A}^{-1}]^T \begin{bmatrix} \frac{\partial \phi}{\partial x} \\ \frac{\partial \phi}{\partial y} \\ \frac{\partial \phi}{\partial z} \end{bmatrix} \end{pmatrix}$$

$$= \mu \mathbf{n}^T \left(-\frac{1}{c} \frac{\partial \phi}{\partial t} \mathbf{M} + (-\mathbf{M} \mathbf{M}^T + \mathbf{I}) \nabla \phi \right) = \mu \left(-\frac{1}{c} M_n \frac{\partial \phi}{\partial t} + (-M_n \mathbf{M}^T + \mathbf{n}^T) \nabla \phi \right)$$

$$= \mu \left(\mathbf{n}^T \nabla \phi - \frac{1}{c} M_n \left(\frac{\partial \phi}{\partial t} + \mathbf{U} \cdot \nabla \phi \right) \right) = \mu \left(\frac{\partial \phi}{\partial n} - \frac{M_n}{c} \frac{D \phi}{D t} \right) = \mu \frac{\partial \phi}{\partial n}, \tag{25}$$

where $\frac{D\phi}{Dt}$ stands for the material time derivative:

$$\frac{D\phi}{Dt} = \frac{\partial\phi}{\partial t} + \mathbf{U} \cdot \nabla\phi \tag{26}$$

and $\frac{\partial \phi}{\partial \hat{n}}$, as denoted in Eq. (25), will be referred to as the *combined normal derivative* [14]:

$$\frac{\partial \phi}{\partial \widetilde{n}} = \frac{\partial \phi}{\partial n} - \frac{M_n}{c} \frac{D\phi}{Dt}.$$
 (27)

Here, $M_n = \mathbf{n} \cdot \mathbf{M}$ is the normal component of the uniform mean flow on solid surfaces, which, because of the uniform mean flow assumption, is not always zero. In fact, M_n is nonzero whenever the assumed constant mean flow is not aligned with the boundary. Clearly, an application of the usual solid surface boundary condition

$$\frac{\partial \phi}{\partial n} = 0 \tag{28}$$

does not lead to as simple a boundary condition for Φ wherever $M_n \neq 0$.

In a recent study in Ref. [14], it was shown that, under the uniform mean flow assumption, instead of the usual boundary condition (28), an alternative Zero Energy Flux (ZEF) boundary condition might be used on solid surfaces:

$$\frac{\partial \phi}{\partial \widetilde{n}} = 0. \tag{29}$$

That is, the boundary condition is such that the combined normal derivative of ϕ is zero. As we will see later, this condition is equivalent to the requirement that the acoustic energy flux be zero at solid surfaces. By Eq. (25), the ZEF boundary condition (29) immediately leads to the following boundary condition in the transformed coordinates:

$$\frac{\partial \Phi}{\partial n'} = 0. \tag{30}$$

Eq. (30) illustrates that, under the ZEF condition, the normal derivative of the velocity potential remains to be zero *when computed in the transformed coordinates*, i.e., the solid wall boundary condition of no flow is preserved under the Prandtl-Glauert-Lorentz transformation. Conversely, Eq. (25) reveals that boundary condition of the form (30) in the transformed coordinates implies the ZEF condition (29) in the physical coordinates.

Therefore, we have shown that the wave scattering problem under a uniform mean flow assumption can be transformed into the standard wave Eq. (18) with the standard solid wall boundary condition (30) in the transformed coordinates. Consequently, methods developed for solving the standard wave equation can be directly applied to the transformed problem. Solutions in the original physical coordinates (x, y, z) and time t can then be found by applying the inverse transform (22) to the results obtained in the transformed coordinates.

We point out that the ZEF condition (29) reduces to the usual solid surface condition (28) wherever $M_n=0$. The fact that the two boundary conditions are different is due to the uniform mean flow assumption which is only an approximation to the actual mean flow when rigid bodies are present. Naturally, as noted in Ref. [14], uniform mean flow assumption would be applicable only to problems where such a simplification is acceptable or justified, such as a flow over slender bodies. According to Eq. (27), the difference between the two boundary conditions is proportional to the normal component of the mean flow at the surface M_n and the time derivative of the solution $\frac{D\phi}{Dt}$. Therefore, at low Mach numbers and low frequencies, or when the assumed mean flow is tangent or nearly tangent to the solid surface, the difference of the two boundary conditions is not expected to be significant. However, as the analysis in this section has shown, when the ZEF condition is used one of the advantages is that the boundary condition in the transformed coordinates becomes significantly simplified.

4. Consequences of the Prandtl-Glauert-Lorentz transformation

In this section, we derive some useful relations for carrying out computations in the transformed domain and for transforming the computational results back to the physical domain.

4.1. Transformation of the source term

To solve the transformed Eq. (18), the source term q(x, y, z, t) of Eq. (1) is also to be transformed into the new coordinates. In this regard, special attention may be needed when transforming point sources defined in delta functions. Consider the case where the source term is of the following form:

$$q(x, y, z, t) = \psi(t)\delta\left(\mathbf{r} - \mathbf{r}_{0}\right) \tag{31}$$

where \mathbf{r}_0 is the location of the point source and $\psi(t)$ is the strength of the source which is assumed to be time dependent. Then, the source term to be used for Eq. (18) in the transformed coordinates becomes the following:

$$Q(x', y', z', t') = \psi \left(\frac{1}{\alpha}t' - \frac{1}{\alpha c}\mathbf{M} \cdot \mathbf{r}'\right) \delta \left(\mathbf{A}^{-1}(\mathbf{r}' - \mathbf{r}'_0)\right)$$

$$= \|\mathbf{A}\|\psi \left(\frac{1}{\alpha}t' - \frac{1}{\alpha c}\mathbf{M} \cdot \mathbf{r}'_0\right) \delta \left(\mathbf{r}' - \mathbf{r}'_0\right)$$
(32)

where $\|A\|$ is the determinant of the spatial transformation matrix A given in Eq. (14) and, consequently, the strength of the point source in the transformed coordinates is modified. Finding the determinant of A by Eq. (14), it can be shown that the modification factor is

$$\|\mathbf{A}\| = \frac{1}{\alpha}.\tag{33}$$

4.2. Transformation of Green's functions

Next, we consider the Green's function for the convective wave Eq. (1). The well-known free-space Green's function for the standard wave Eq. (18) in the transformed coordinates defined by

$$\frac{\partial^2 G}{\partial t'^2} - c^2 \nabla'^2 G = \delta(t' - t'_0) \delta(\mathbf{r}' - \mathbf{r}'_0) \tag{34}$$

is the following,

$$G(\mathbf{r}', t'; \mathbf{r}'_0, t'_0) = \frac{\delta\left(t' - t'_0 - |\mathbf{r}' - \mathbf{r}'_0|/c\right)}{4\pi c^2 \left|\mathbf{r}' - \mathbf{r}'_0\right|}$$
(35)

where \mathbf{r}_0' and \mathbf{t}_0' denote, respectively, the source point and initial time for the Green's function. To transform the above back to the one in the physical coordinates \mathbf{r} and t, using Eq. (16), we note

$$\left| \mathbf{r}' - \mathbf{r}'_0 \right|^2 = \left(\mathbf{r} - \mathbf{r}_0 \right)^T \mathbf{A}^T \mathbf{A} \left(\mathbf{r} - \mathbf{r}_0 \right) = \left(\mathbf{r} - \mathbf{r}_0 \right)^T \left(\frac{1}{\alpha^2} \mathbf{M} \mathbf{M}^T + \mathbf{I} \right) \left(\mathbf{r} - \mathbf{r}_0 \right) = \frac{\overline{R}^2}{\alpha^2}$$

where

$$\overline{R} = \sqrt{\left| \mathbf{M} \cdot (\mathbf{r} - \mathbf{r}_0) \right|^2 + \alpha^2 \left| \mathbf{r} - \mathbf{r}_0 \right|^2} \tag{36}$$

and

$$\delta\left(t'-t_0'-|\mathbf{r'}-\mathbf{r'_0}|/c\right) = \frac{1}{\alpha}\delta\left(t-t_0+\frac{1}{\alpha^2c}\left(\mathbf{M}\cdot\left(\mathbf{r}-\mathbf{r_0}\right)\right)-\frac{\overline{R}}{\alpha^2c}\right),$$

giving the Green's function in the physical coordinates for the convective wave Eq. (1) as

$$g(\mathbf{r},t;\mathbf{r}_{0},t_{0}) = \frac{\delta\left(t-t_{0} + \frac{1}{\alpha^{2}c}\left(\mathbf{M}\cdot(\mathbf{r}-\mathbf{r}_{0})\right) - \frac{\overline{R}}{\alpha^{2}c}\right)}{4\pi c^{2}\overline{R}},$$
(37)

where $g(\mathbf{r}, t; \mathbf{r}_0, t_0)$ satisfies

$$\left(\frac{\partial}{\partial t} + \boldsymbol{U} \cdot \nabla\right)^2 g - c^2 \nabla^2 g = \delta(t - t_0) \delta\left(\boldsymbol{r} - \boldsymbol{r}_0\right). \tag{38}$$

4.3. Transformation of the energy equation

We further consider transformation of the energy equation. The well-known energy equation for the standard wave Eq. (18) with a homogeneous source term is

$$\frac{\partial E'}{\partial t'} + \nabla' \cdot \mathbf{J}' = 0 \tag{39}$$

where

$$E' = \frac{1}{2} |\nabla' \Phi|^2 + \frac{1}{2c^2} \left| \frac{\partial \Phi}{\partial t'} \right|^2, \quad \mathbf{J}' = -\frac{\partial \Phi}{\partial t'} \nabla' \Phi \tag{40}$$

It is straightforward to find that, when expressed in the original physical coordinates (x, y, z) and time t, we have

$$E' = \frac{1}{\alpha^2 c^2} \left| \frac{\partial \phi}{\partial t} \right|^2 - \frac{1}{c^2} \frac{\partial \phi}{\partial t} \frac{D\phi}{Dt} + E \tag{41}$$

and

$$\nabla' \cdot \mathbf{J}' = -\frac{1}{\alpha} \frac{\partial}{\partial t} \left(\frac{1}{\alpha^2 c^2} \left| \frac{\partial \phi}{\partial t} \right|^2 - \frac{1}{c^2} \frac{\partial \phi}{\partial t} \frac{D\phi}{Dt} \right) + \frac{1}{\alpha} \nabla \cdot \mathbf{J}$$
(42)

where

$$E = \frac{1}{2} |\nabla \phi|^2 + \frac{1}{2c^2} \left| \frac{D\phi}{Dt} \right|^2 - \frac{\mathbf{M} \cdot \nabla \phi}{c} \frac{D\phi}{Dt}, \quad \mathbf{J} = -\frac{\partial \phi}{\partial t} \left(\nabla \phi - \frac{1}{c} \frac{D\phi}{Dt} \mathbf{M} \right). \tag{43}$$

By substituting Eqs. (41) and (42) into Eq. (39), we get the following conservation equation for the convective wave Eq. (1):

$$\frac{\partial E}{\partial t} + \nabla \cdot \boldsymbol{J} = 0,\tag{44}$$

where E and J are as given in Eq. (43). When substituted by the acoustic pressure and velocity, Eq. (44) is equivalent to the familiar energy equation for acoustic waves in a uniform flow with $\rho_0 E$ as the acoustic energy density [19,20,22]. Furthermore, using Eq. (43), it is easily found that energy flux through a surface of normal n is

$$\mathbf{J} \cdot \mathbf{n} = -\frac{\partial \phi}{\partial t} \left(\frac{\partial \phi}{\partial n} - \frac{M_n}{c} \frac{D\phi}{Dt} \right) = -\frac{\partial \phi}{\partial t} \frac{\partial \phi}{\partial \tilde{n}}$$

$$\tag{45}$$

Note that the energy flux is directly proportional to the combined normal derivative of ϕ as defined in Eq. (27). Obviously, the ZEF boundary condition as stated in Eq. (29) satisfies the requirement that $\mathbf{J} \cdot \mathbf{n} = 0$ on solid surfaces, i.e., the energy flux being zero. On the other hand, as noted in Ref. [14], the usual solid surface condition (28) will result in nonzero energy flux wherever M_n is nonzero.

4.4. Finding acoustic pressure and velocity

To find the acoustic pressure and velocity in the physical space from the velocity potential Φ that is computed in the transformed coordinates, we have

$$p(x, y, z, t) = -\rho_0 \left(\frac{\partial \boldsymbol{\phi}}{\partial t} + \boldsymbol{U} \cdot \nabla \boldsymbol{\phi} \right) = -\rho_0 \left(\alpha \frac{\partial \boldsymbol{\Phi}}{\partial t'} + \boldsymbol{U}^T \begin{bmatrix} \boldsymbol{b} & \boldsymbol{A}^T \end{bmatrix} \begin{bmatrix} \frac{\partial \boldsymbol{\Phi}}{\partial t'} \\ \frac{\partial \boldsymbol{\Phi}}{\partial x'} \\ \frac{\partial \boldsymbol{\Phi}}{\partial y'} \\ \frac{\partial \boldsymbol{\Phi}}{\partial z'} \end{bmatrix} \right)$$

$$= -\rho_0 \left(\alpha \frac{\partial \Phi}{\partial t'} + \mathbf{U}^T \mathbf{b} \frac{\partial \Phi}{\partial t'} + \mathbf{U}^T \mathbf{A}^T \middle| \frac{\partial \Phi}{\partial y'} \middle| \frac{\partial \Phi}{\partial z'} \middle| \right) = -\frac{\rho_0}{\alpha} \left(\frac{\partial \Phi}{\partial t'} + \mathbf{U} \cdot \nabla' \Phi \right)$$

$$(46)$$

and

$$\mathbf{u}(x, y, z, t) = \nabla \phi = \frac{\mathbf{M}}{\alpha c} \frac{\partial \Phi}{\partial t'} + \mathbf{A}^T \nabla' \Phi$$
(47)

where relations shown in Eqs. (12) and (20) have been used.

4.5. Transformation of frequency domain solutions

The frequency domain solutions in the two coordinates are also related. Let the frequency domain solution in transformed space-time coordinates (x', y', z', t') be defined as

$$\widehat{\Phi}(x', y', z', \omega') = \int_{-\infty}^{\infty} \Phi(x', y', z', t') e^{i\omega't'} dt'. \tag{48}$$

where a hat indicates the frequency domain solution. Then, using Eq. (15), it follows that

$$\begin{split} \widehat{\Phi}(x',y',z',\omega') &= \alpha \int_{-\infty}^{\infty} \Phi(x',y',z',t') e^{i\omega'\alpha t} e^{\frac{i\omega'}{\alpha c} \left(M_1 x + M_2 y + M_3 z\right)} dt \\ &= \alpha e^{\frac{i\omega'}{\alpha c} \left(M_1 x + M_2 y + M_3 z\right)} \int_{-\infty}^{\infty} \phi(x,y,z,t) e^{i\omega'\alpha t} dt = \alpha e^{\frac{i\omega'}{\alpha c} \left(M_1 x + M_2 y + M_3 z\right)} \widehat{\phi}(x,y,z,\omega'\alpha) \end{split}$$

or, equivalently, for the frequency domain solution in the physical coordinates,

$$\widehat{\phi}(x,y,z,\omega) = \frac{1}{\alpha} \widehat{\Phi}(x',y',z',\omega') e^{-\frac{i\omega}{\alpha^2 c} (M_1 x + M_2 y + M_3 z)}$$
(49)

where

$$\omega = \alpha \omega' \tag{50}$$

is the relation between the frequencies in the two coordinates.

5. Numerical examples

Given the simplicity of the standard wave equation, it would be advantageous to solve the convective wave Eq. (1) by first applying the Prandtl-Glauert-Lorentz transformation to Eq. (1) and then transforming the solution back to the physical coordinates. It should be pointed out that a fixed time in t does not lead to a fixed time in t' when spatial coordinates are varying. For acoustic problems, however, often only the solutions in frequency domain are of interest. For such cases, the frequency domain solutions of the transformed and the original space-time coordinates are directly related through the relations developed in Sec. 4.5.

In this section, two numerical examples are presented. In the first example, acoustic scattering of a point source by a parabolic wing section is solved first in the transformed coordinates and then transformed back to obtain the solution in the original physical coordinates. In the second example, numerical solution by the ZEF condition under a uniform mean flow assumption is compared with that by the linearized Euler equations under a potential mean flow assumption.

5.1. Scattering by a parabolic wing section

We present a numerical example of solving the convective wave equation in the transformed coordinates using a Time Domain Boundary Element Method (TDBEM) [14]. It is well-known that the standard wave Eq. (18) coupled with solid wall boundary condition (30) can be converted into a Time Domain Boundary Integral Equation (TDBIE) as follows:

$$2\pi\Phi(\overline{\mathbf{r}}_{s}',\overline{\mathbf{t}}') + \int_{S'} \frac{\partial G_{0}}{\partial n'} \left(\Phi(\mathbf{r}_{s}',\overline{\mathbf{t}}_{R}') + \frac{R(\mathbf{r}_{s}',\overline{\mathbf{r}}_{s}')}{c} \frac{\partial \Phi}{\partial t}(\mathbf{r}_{s}',\overline{\mathbf{t}}_{R}') \right) d\mathbf{r}_{s}' = \frac{1}{c^{2}} \int_{V_{s}'} \frac{1}{R(\mathbf{r}',\overline{\mathbf{r}}_{s}')} Q(\mathbf{r}',\overline{\mathbf{t}}_{R}') d\mathbf{r}'$$

$$(51)$$

where \mathbf{r}'_s and \mathbf{r}' denote, respectively, the integration variables on the transformed surface S' and volume source region V'_s in the transformed (x', y', z') coordinates, and R denotes their distances to the collocation point denoted as $\overline{\mathbf{r}}'_s$ (assumed here to be a smooth surface point) and \overline{t}'_p is the retarded time:

$$R(\mathbf{r}'_{s}, \overline{\mathbf{r}}'_{s}) = |\overline{\mathbf{r}}'_{s} - \mathbf{r}'_{s}|, \quad \overline{t}'_{R} = \overline{t}' - \frac{R(\mathbf{r}'_{s}, \overline{\mathbf{r}}'_{s})}{c}, \quad G_{0} = \frac{1}{R(\mathbf{r}'_{s}, \overline{\mathbf{r}}'_{s})}$$

$$(52)$$

The boundary element method for Eq. (51) involves an expansion of the unknown function $\Phi(\mathbf{r}'_s, t')$ in spatial and temporal basis functions and a solution of the linear algebraic system formed by substituting the expansion into Eq. (51) and forcing the equation to be satisfied at a set of collocation points, leading to a March-On-in-Time (MOT) scheme. Further details on the numerical method used for the example are referred to Ref. [14].

To validate the conversion of the convective wave equation by the Prandtl-Glauert-Lorentz transformation and the equivalence of the frequency domain solutions shown in Sec. 4.5, we present a numerical example of sound scattering by a section of parabolic wing in the presence of a uniform mean flow. The computations are done with and without the Prandtl-Glauert-Lorentz transformation and the frequency domain results by the two approaches will be compared. The computation without the Prandtl-Glauert-Lorentz transformation is done by solving the TDBIE derived directly from the convective wave Eq. (1), as detailed in Ref. [14]. For references, formulation for the direct boundary integral equation in physical coordinates is given in the Appendix.

The geometry of the scattering surface is that of a convex parabolic wing section. The upper and lower surfaces of the body are defined as follows:

$$z = \pm 0.1 L_{x} (1 - x^{2} / L_{y}^{2}), \quad -L_{x} \le x \le L_{x}, \quad -L_{y} \le y \le L_{y}$$
(53)

where $L_x = L_y = 0.5$. In this example, the scattering surface is discretized by 8896 unstructured triangular elements and each is in turn subdivided into three quadrilateral elements, yielding a total of 26688 elements. The source function as it appears in (1) is a broadband point source defined as the following:

$$q(\mathbf{r},t) = e^{-\sigma t^2} \delta(\mathbf{r} - \mathbf{r}_0)$$
(54)

where the location of source point $\mathbf{r}_0 = (0, 0, 0.5)$, and $\sigma = 1.42/(6\Delta t)^2$. For the computational results reported below, the non-dimensional time step is $c\Delta t/L_x = 0.025$. The Mach number of the mean flow is $\mathbf{M} = (0.5, 0, 0)$.

In Fig. 1, the geometric setup for computing the scattering of a point source by a section of parabolic wing is shown on the left in the physical coordinates and an instantaneous pressure contour plot of the TDBEM solution is shown on the right in the transformed coordinates. As the time domain computation is carried out in the transformed coordinates, the body of the scatterer is stretched by a factor of $1/\alpha$ along the direction of the flow according to Eq. (15).

Once the simulation in the time domain is completed, frequency domain solutions can be obtained by an application of FFT (Fast Fourier Transform) to the solution, or by the following summation for a selected set of frequencies of interest:

$$\widehat{\Phi}(\mathbf{r}',\omega') = \Delta t' \left[\Phi(\mathbf{r}',t_1')e^{-i\omega't_1'} + \Phi(\mathbf{r}',t_2')e^{-i\omega't_2'} + \Phi(\mathbf{r}',t_3')e^{-i\omega't_3'} + \dots + \Phi(\mathbf{r}',t_{N_t}')e^{-i\omega't_{N_t}'} \right]$$

$$(55)$$

where $\Delta t'$ is the time step of the TDBEM scheme applied in the transformed coordinates and N_t is the total number of time steps. Frequency domain solutions in the physical coordinates $\hat{\phi}(\mathbf{r},\omega)$ can be found by applying the inverse transform (22) for the coordinates and by the relations shown in Sec. 4.5. In Fig. 2, solutions at two frequencies, $kL_x = 5$ and 10 where $k = \omega/c$, are shown for the contours of the real part of $\hat{\phi}(\mathbf{r},\omega)$ on the field points and on the scattering surface. The mean flow effects on the scattered waves in the physical coordinates are clearly seen.

Moreover, solutions along a field line located at y=0, z=-2.0 and for $-2.0 \le x \le 2.0$ are plotted in Fig. 3 as a function of x. Also plotted are the solution obtained without using the Prandtl-Glauert-Lorentz transformation, i.e., by solving the time domain integral equation formulated directly from the convective wave Eq. (1) as discussed in Ref. [14]. Results from the two approaches are in very good agreement. While the results in Fig. 3 confirm the equivalence of frequency domain solutions by the two approaches, numerical solution by using the transformed equation is preferred because of the simpler integral kernel encountered in Eq. (51) as compared to the integral kernel for Eq. (1) as shown in the Appendix. Another advantage in solving the equation in the transformed coordinates is that the mean flow effect on the wave speeds of the upstream and downstream propagating waves is avoided. As a result, computational time for the pulse to propagate through the entire computational

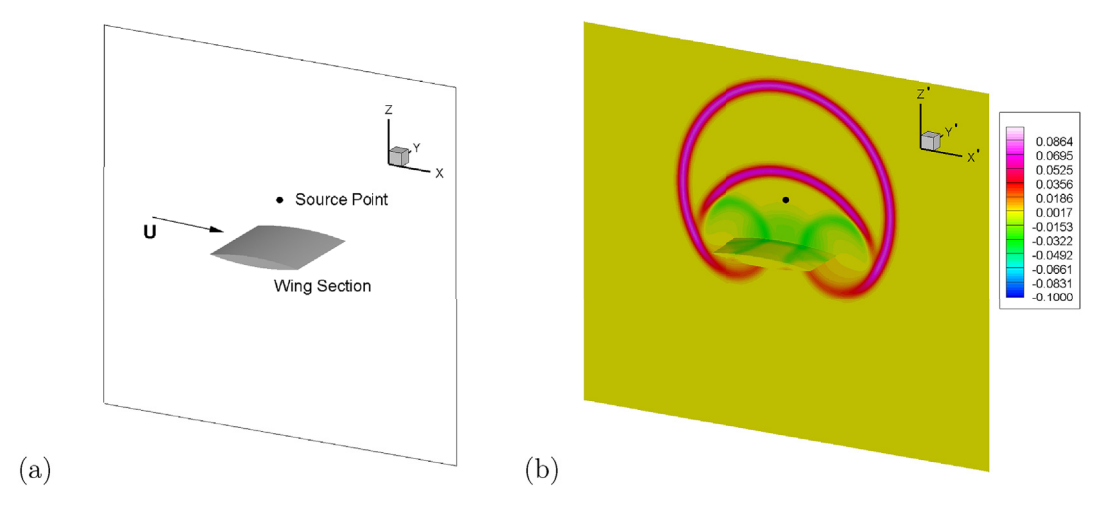


Fig. 1. (a): A schematic of geometrical setup for the scattering surface and location of point source; (b): instantaneous contours of ϕ by TDBEM computed in the transformed space-time coordinates (x', y', z', z'). The scattering surface is stretched by a factor of $1/\alpha$ in the direction of the mean flow.

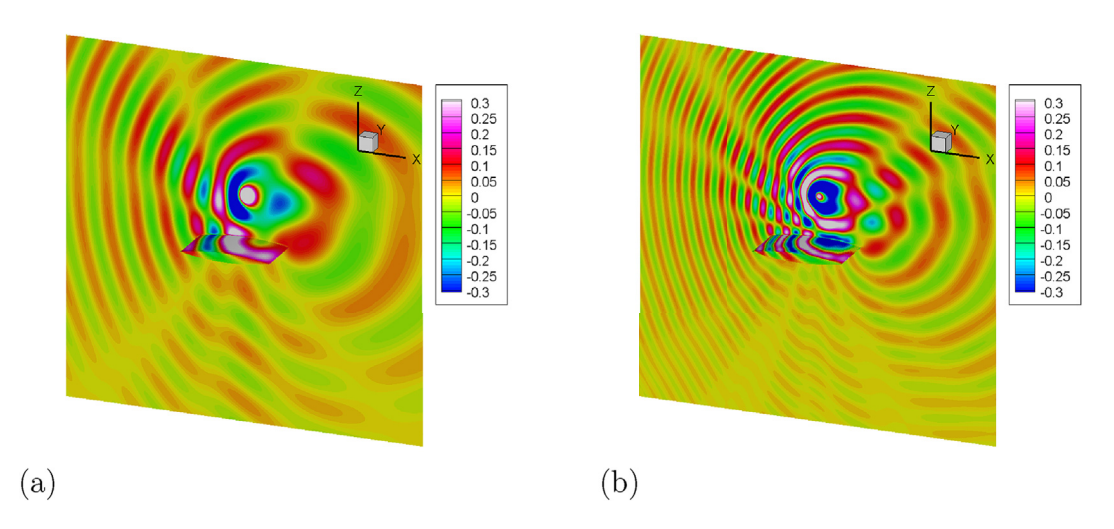


Fig. 2. Contours of the frequency domain solution in the physical coordinates (x, y, z, t) transformed back from the results computed in (x', y', z', t'). (a) $kL_x = 5$; (b) $kL_x = 10$, where $k = \omega/c$.

domain is shortened compared to the case without the Prandtl-Glauert-Lorentz transformation. For the current example, using a criterion that numerical simulation is ended when the acoustic pulse has propagated through all the field points and the magnitude of the solution at all field points is less than 10^{-6} , the total number of time steps N_t used is 775 and 982 respectively for the computation with and without the Prandtl-Glauert-Lorentz transformation. This is a substantial gain in efficiency for using the Prandtl-Glauert-Lorentz transformation.

5.2. Scattering by a sphere with potential flow

In the second example, we compare the numerical solution for the scattering of a point source by a solid body obtained under a uniform mean flow assumption with that under a nonuniform potential flow assumption. Also included in the comparison is the solution by the conventional solid wall condition under the uniform mean flow assumption, referred to as the zero normal velocity (ZNV) condition in this section. As pointed out earlier, the ZEF condition differs from the conventional ZNV condition where $M_n \neq 0$, i.e., when the uniform flow assumption itself does not satisfy the solid surface condition. Of course the two conditions become the same when $M_n = 0$ as Eq. (27) shows. A potential flow that does satisfy the solid surface condition everywhere is a more realistic mean flow to use. By comparing the solutions by both the ZEF and ZNV conditions of uniform mean flow with that of the nonuniform potential flow, the accuracy and adequacy of the ZEF condition may be assessed. The solid body is chosen to be a sphere where an analytical expression for the potential flow is readily available. The solution for the

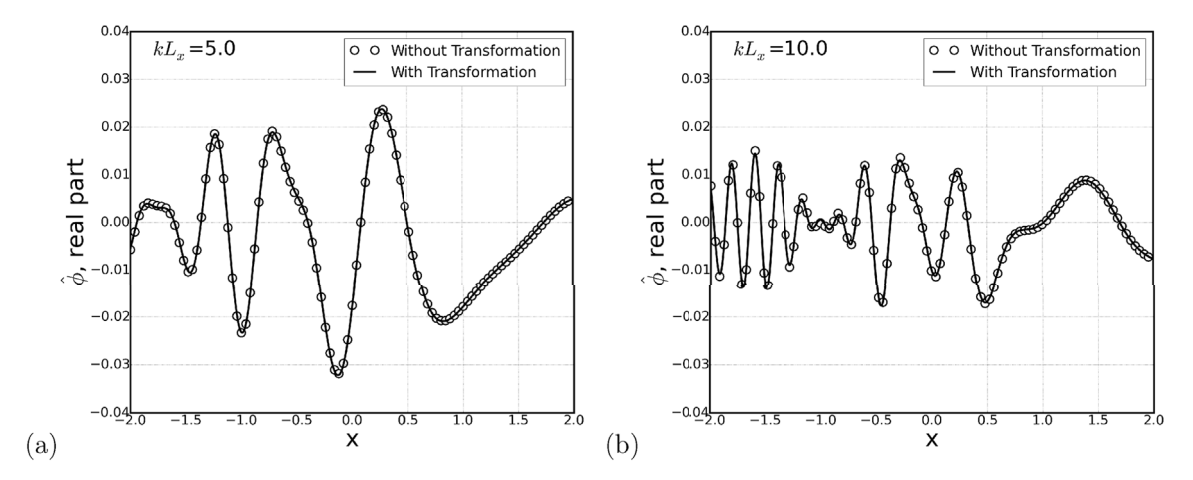


Fig. 3. Frequency domain solution along a field line located at y=0, z=-2.0 and for $-2.0 \le x \le 2.0$. Plotted are the real part of $\hat{\phi}$. Computations performed by using the Prandtl-Glauert-Lorentz transformation are shown in lines and without the transformation are in symbols. (a) $kL_v=5$; (b) $kL_v=10$, where $k=\omega/c$.

scattering by the nonuniform potential flow will be found by solving the linearized Euler equations.

The velocity field of a potential flow past a stationary sphere of radius *a* and centered at the origin is well-known [3]:

$$\mathbf{U}_0 = \nabla \phi_0, \quad \phi_0 = U_\infty x \left(1 + \frac{a^3}{2(x^2 + y^2 + z^2)^{3/2}} \right)$$
 (56)

where $\mathbf{U} = (U_{\infty}, 0, 0)$ is the external uniform mean flow far away from the sphere. Unlike the simplified uniform mean flow, the potential mean flow satisfies the solid surface boundary condition everywhere on the sphere. An example of the streamwise velocity is shown in Fig. 4 (a) for the case of Mach number $M = U_{\infty}/c = 0.2$. For the current example, the radius of sphere a = 0.5 and its diameter d = 2a = 1.

The following linearized Euler equations are solved with a point source of the same form as in (54):

$$\frac{\partial \mathbf{u}}{\partial t} + (\mathbf{U}_0 \cdot \nabla) \mathbf{u} + (\mathbf{u} \cdot \nabla) \mathbf{U}_0 + \frac{1}{\rho_0} \nabla p = 0$$
 (57)

$$\frac{\partial p}{\partial t} + \boldsymbol{U}_0 \cdot \nabla p + \gamma P_0(\nabla \cdot \boldsymbol{u}) + \gamma (\nabla \cdot \boldsymbol{U}_0) p = -\rho_0 q(\boldsymbol{r}, t)$$
(58)

The mean density ρ_0 and mean pressure P_0 are assumed to be constant, and their relation with the acoustic wave speed is $c = \sqrt{\gamma P_0/\rho_0}$, $\gamma = 1.4$. Eqs. (57) and (58) reduce to the convective wave equation under a uniform mean flow assumption as given in Eqs. (1) and (3). For the current example, the point source is located at $\mathbf{r}_0 = (0, 0, 1.5)$.

The Euler equations are solved numerically by a time domain finite difference overset grid method [25]. The computational domain of $[-3,3] \times [-3,3] \times [-3,3]$ is discretized using a Cartesian finite difference grid of spacing $\Delta x = \Delta y = \Delta z = 0.03$

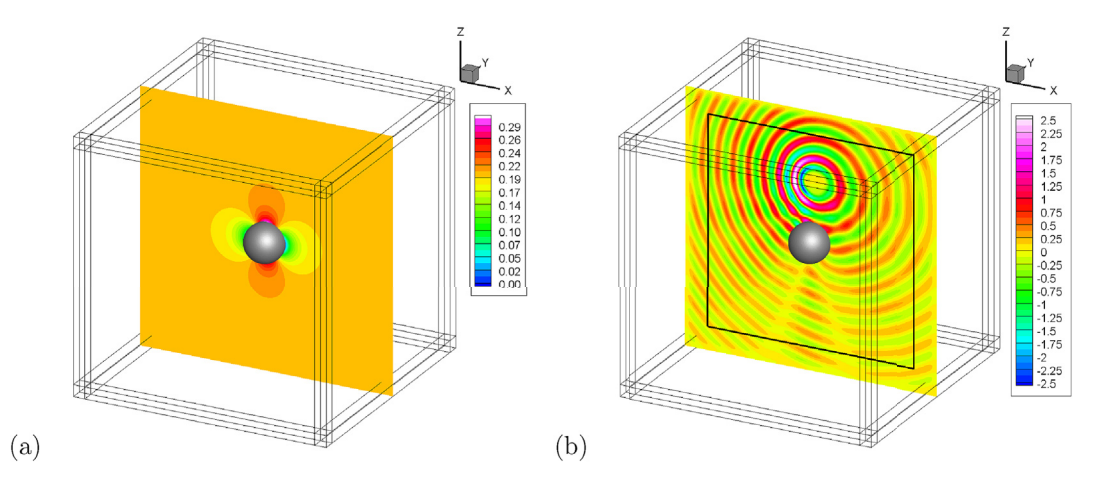


Fig. 4. Diagrams of the three-dimensional computational domain terminated by Perfectly Match Layers (PML). (a): Contours of streamwise velocity of the potential mean flow past a sphere of radius a=0.5, with Mach number $U_{\infty}/c=0.2$; (b): Converted frequency domain solution, for the real part of $\hat{p}(\mathbf{r},\omega)$, of scattering by the sphere for a point source located at (0,0,1.5), $\omega d/c=4\pi$. Dark solid lines indicate locations where solutions are compared in Fig. 5.

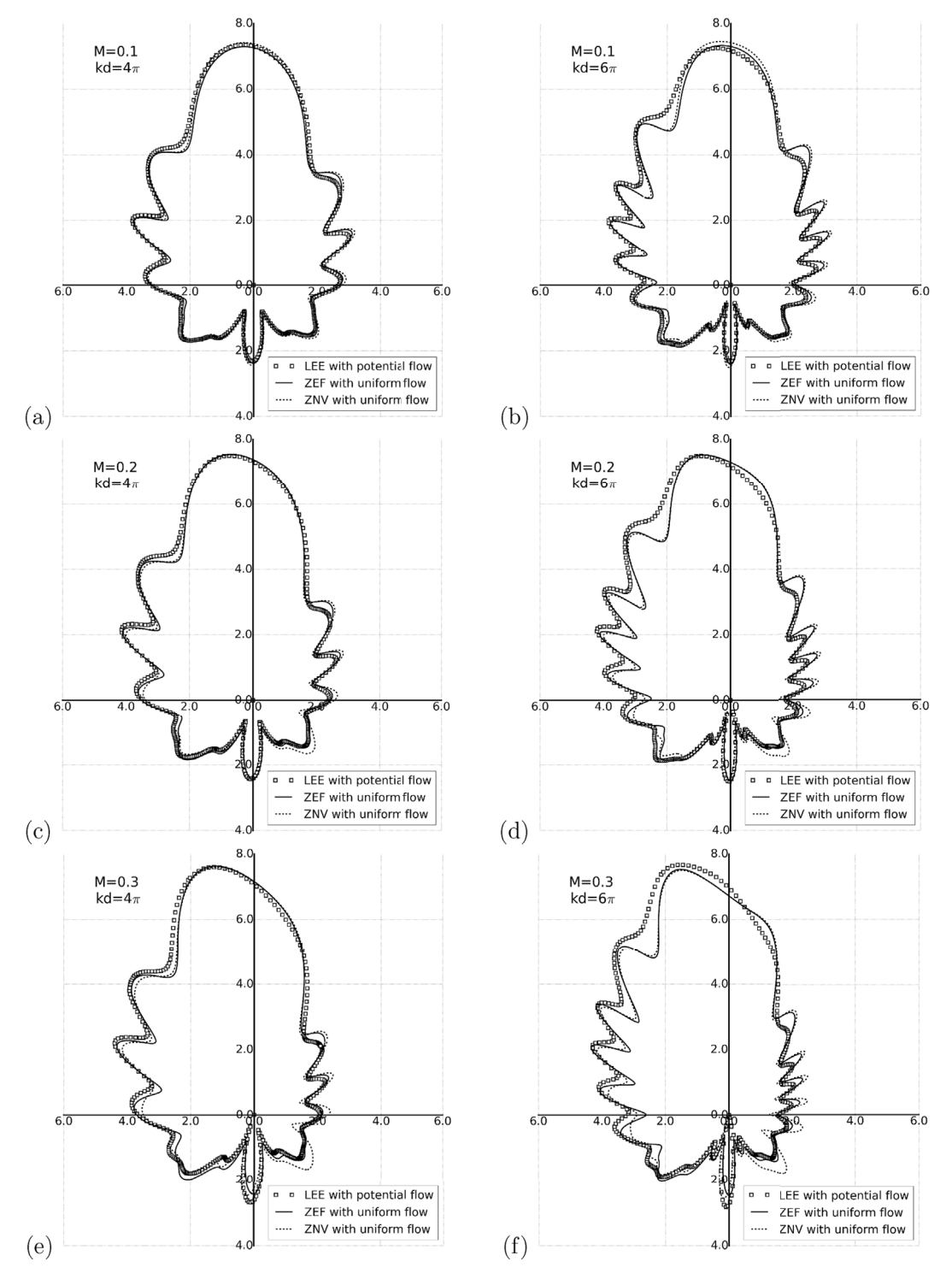


Fig. 5. Directivity plots of $D(\theta)$ for solutions by the linearized Euler equation (LEE) with nonuniform potential mean flow (symbols), ZEF condition with a uniform mean flow (solid), and ZNV condition with a uniform mean flow (dash). $k = \omega/c$ and d = 2a. (a) M = 0.1, $kd = 4\pi$; (b) M = 0.1, $kd = 6\pi$; (c) M = 0.2, $kd = 4\pi$; (d) M = 0.2, $kd = 6\pi$.

and body fitted grid zones based on the spherical coordinates around the sphere, with a total of over 17 million grid points. For the solution of the Euler equations with the potential mean flow, the usual solid wall condition, i.e., $\mathbf{n} \cdot \mathbf{u} = 0$, is applied on the surface of the sphere. The computational domain is terminated at the non-reflecting far-field boundary by applying the Perfectly Matched Layer (PML) absorbing boundary condition [13], as illustrated in Fig. 4. Spatial derivatives are approximated by the

7-point 4th-order central differences (DRP scheme) [26], and time integration is carried out by 4th-order optimized Runge-Kutta scheme (LDDRK56) [11]. Further details on the overset numerical method are referred to Ref. [25].

Also shown in Fig. 4 (b) is a contour plot of the converted frequency domain solution at $\omega d/c = 4\pi$. The frequency domain solution is obtained from the time domain solution of the linearized Euler equations by a postprocessing procedure as described in (55).

In Fig. 5, we present the comparison of the solution computed by the linearized Euler equations with a potential mean flow and that of the ZEF condition (29) and the ZNV condition (28) with a uniform mean flow both computed by the TDBIE approach. For the solution of the TDBIE, the surface of the sphere is discretized by 1536 constant elements. While the pressure in the solution of the linearized Euler equations is computed directly, the pressure by the solution of integral equations for the acoustics velocity potential is computed using the relation given in (46). The frequency domain pressure $\hat{p}(\mathbf{r}, \omega)$ of the three solutions along the four field lines of $x = \pm 2.7$ and $z = \pm 2.7$ on the plane y = 0, as indicated in Fig. 4 (b), are plotted in Fig. 5 as polar graphs of non-dimensional directivity functions defined as follows:

$$D(\theta) = \frac{|\mathbf{r}|}{d} \left| \frac{\widehat{p}(\mathbf{r}, \omega)}{\widehat{p}_0(\omega)} \right|$$
 (59)

where d=2a is the diameter of the sphere and $\hat{p}_0(\omega)$ denotes the reference value taken to be the pressure of the point source (without the body) at the center of the sphere (0,0,0).

The results for three cases of mean flow Mach numbers $M=U_{\infty}/c=0.1,\,0.2,\,$ and 0.3 and at two frequencies $\omega d/c=4\pi$ and 6π are shown in Fig. 5. The solutions by the nonuniform potential mean flow are shown in symbols, and the solutions by the uniform mean flow assumption with ZEF and ZNV conditions are shown respectively in solid and dashed lines. Fig. 5 shows that, while it is expected that the solutions computed under the uniform mean flow assumption will deviate from that computed using the nonuniform potential mean flow, the solution by the ZEF condition is seen to be closer to that by the potential flow in this example. At low Mach number and low frequency, the difference between the solutions by the ZEF and ZNV conditions is relatively small. The difference increases when the Mach number and frequency are increased. This is consistent with the expression given in (27) which shows that the difference of the two boundary conditions, (28) and (29), is proportional to M_n and $\frac{D\phi}{Dc}$.

6. Conclusions

A study of the solid surface boundary condition to be used under the Prandtl-Glauert-Lorentz transformation for the convective wave equation has been presented. It has been shown that with an application of the recently proposed ZEF solid surface condition, the boundary condition that the normal derivative of the velocity potential be zero for the case of no flow remains so when computed in the transformed coordinates. As such, the solid wall boundary condition of no flow is preserved using the Prandtl-Glauert-Lorentz transformation with the ZEF condition. This observation points to an attractive alternative for solving the problem of acoustic scattering by rigid bodies in the presence of a uniform mean flow, particularly for the methods based on the boundary element methods, because of the simplified kernel function in the transformed coordinates, for both the time domain and the frequency domain approaches. Numerical examples are also presented that demonstrate the utility of the Prandtl-Glauert-Lorentz transformation.

Acknowledgments

F. Q. Hu and M. E. Pizzo are supported by a NASA Cooperative Agreement, NNX11Al63A. M. E. Pizzo is also supported in part by an Old Dominion University Modeling and Simulation graduate fellowship. This work used the computational resources at the Old Dominion University ITS Turing cluster and the Extreme Science and Engineering Discovery Environment (XSEDE), which is supported by National Science Foundation grant number OCI-1053575. The authors thank the anonymous reviewers for constructive comments and suggestions.

Appendix

In this appendix, we show briefly the integral equation formulation in the physical coordinates. The time domain boundary integral equation in the physical coordinates for the convective wave Eq. (1) can be written as follows [14]:

$$2\pi\phi(\overline{\boldsymbol{r}}_{s},\overline{t}) - \int_{S} \left(G_{0} \frac{\partial \phi}{\partial \overline{n}}(\boldsymbol{r}_{s},\overline{t}_{R}) - \frac{\partial G_{0}}{\partial \overline{n}} \left[\phi(\boldsymbol{r}_{s},\overline{t}_{R}) + \frac{\overline{R}}{c\alpha^{2}} \frac{\partial \phi}{\partial t}(\boldsymbol{r}_{s},\overline{t}_{R}) \right] \right) d\boldsymbol{r}_{s} = \overline{q}(\overline{\boldsymbol{r}}_{s},\overline{t})$$

$$(60)$$

where $\overline{q}(\overline{r}_s, \overline{t})$ is the contribution from the external sources to a surface collocation point denoted as \overline{r}_s :

$$\overline{q}(\overline{r}_{s},\overline{t}) = \frac{1}{c^{2}} \int_{V_{c}} \frac{1}{R} q(\mathbf{r},\overline{t}_{R}) d\mathbf{r}$$
(61)

and

$$\overline{t}_R = \overline{t} + \boldsymbol{\beta} \cdot (\overline{\boldsymbol{r}} - \boldsymbol{r}) - \frac{\overline{R}}{c\alpha^2}, \quad \overline{R} = \sqrt{\left[\boldsymbol{M} \cdot (\boldsymbol{r} - \overline{\boldsymbol{r}})\right]^2 + \alpha^2 |\boldsymbol{r} - \overline{\boldsymbol{r}}|^2}, \text{ and } G_0 = \frac{1}{R}$$
 (62)

in which

$$\mathbf{M} = \frac{\mathbf{U}}{c}, \ \alpha = \sqrt{1 - M^2}, \ \boldsymbol{\beta} = \frac{\mathbf{U}}{c^2 - U^2} = \frac{\mathbf{U}}{c^2 \alpha^2} = \frac{\mathbf{M}}{c \alpha^2}, \ U = |\mathbf{U}|, \ M = |\mathbf{M}|$$
 (63)

The combined normal derivative $\partial \phi / \partial \widetilde{n}$ appearing in (60) is as defined in (27) and the modified normal derivative for G_0 appearing in (60) is defined as follows:

$$\frac{\partial G_0}{\partial \overline{n}} = \frac{\partial G_0}{\partial n} - M_n(\mathbf{M} \cdot \nabla G_0) \tag{64}$$

The ZEF boundary condition for ϕ on solid surfaces in physical coordinates is that of (29):

$$\frac{\partial \phi}{\partial \widetilde{n}} = 0$$

To effectively suppress the well-known instability associated with the exterior scattering problem, a Burton-Miller type reformulation is applied to the integral Eq. (60) [5,14]. The Burton-Miller reformulation involves applying the following operator:

$$\frac{\partial}{\partial \overline{t}} - c \frac{\partial}{\partial \widetilde{n}} \tag{65}$$

to the integral equation (60) to eliminate the non-trivial resonant solutions contained in (60). Further details are referred to Ref. [14].

References

- [1] R. Amiet, W.R. Sears, The aerodynamic noise of small-perturbation subsonic flows, J. Fluid Mech. 44 (1970) 227-235.
- [2] R.J. Astley, J.G. Bain, A three-dimensional boundary element scheme for acoustic radiation in low Mach number flows, J. Sound Vib. 109 (1986) 445–465.
- [3] G.K. Batchelor, An Introduction to Fluid Dynamics, Cambridge University Press, 1967.
- [4] A. Bayliss, E. Turkel, Far field boundary conditions for compressible flows, J. Comput. Phys. 48 (1982) 182–199.
- [5] A.J. Burton, G.F. Miller, The application of integral equation methods to the numerical solution of some exterior boundary-value problems, Proc. R. Soc. London, Ser A 323 (1971) 201–210.
- [6] N. Balin, F. Casenave, F. Dubois, E. Duceau, S. Duprey, I. Terrasse, Boundary element and finite element coupling for aeroacoustics simulations, J. Comput. Phys. 294 (2015) 274–296.
- [7] C.J. Chapman, Similarity variables for sound radiation in a uniform flow, J. Sound Vib. 233 (2000) 157–164.
- [8] M. Gennaretti, C. Testa, Boundary integral formulation for sound scattered by moving bodies, J. Sound Vib. 314 (2008) 712–737.
- [9] H. Glauert, The effect of compressibility on the lift of an airfoil, Proc. R. Soc. Lond. CXVIII (1928) 113–119.
- [10] A.L. Gregory, S. Sinayoko, A. Agarwal, J. Lasenby, An acoustic space-time and the Lorentz transformation in aeroacoustics, Int. J. Aeroacoustics 14 (2015) 977–1003.
- [11] F.Q. Hu, M.Y. Hussaini, J.L. Manthey, Low-dissipation and low-dispersion Runge-Kutta schemes for computational acoustics, J. Comput. Phys. 124 (1996) 177–191.
- [12] F.Q. Hu, A stable, perfectly matched layer for linearized Euler equations in unsplit physical variables, J. Comput. Phys. 173 (2001) 455-480.
- [13] F.Q. Hu, Absorbing boundary conditions, Int. J. Comput. Fluid Dynam. 18 (2004) 513-522.
- [14] F.Q. Hu, M.E. Pizzo, D.M. Nark, On a time domain boundary integral equation formulation for acoustic scattering by rigid bodies in uniform mean flow, J. Acoust. Soc. Am. 142 (2017) 3624–3636.
- [15] J.D. Jackson, Classical Electrodynamics, third ed., Wiley, 1998.
- [16] H.G. Kussner, General Airfoil Theory, NACA Tech. Memo., No. 979, 1941.
- [17] S. Mancini, R.J. Astley, S. Sinayoko, G. Gabard, M. Tournour, Assessment of the Taylor-Lorentz Transform for Boundary Element Solutions to Wave Propagation with Mean Flow, AIAA paper 2017-3512, 2017.
- [18] J.W. Miles, On the compressibility correction for subsonic unsteady flow, J. Aeronaut. Sci. 17 (1950) 181–182.
- [19] W. Mohring, Energy conservation, time reversal invariance and reciprocity in ducts with flow, J. Fluid Mech. 431 (2001) 223–237.
- [20] C.L. Morfey, Acoustic energy in non-uniform flows, J. Sound Vib. 14 (1971) 159–179.
- [21] P.M. Morse, K.U. Ingard, Theoretical Acoustics, Princeton University Press, 1987.
- [22] M.K. Myers, Transport of energy by disturbances in arbitrary flows, J. Fluid Mech. 226 (1991) 383–400.
- [23] D. Papamoschou, S. Mayoral, Modeling of Jet Noise Sources and Their Diffraction with Uniform Flow, AIAA paper 2013-0326, 2013.
- [24] W.R. Sears, Small-perturbation Theory, Princeton University Press, 1960.
- [25] C.K.W. Tam, F.Q. Hu, An Optimized Multi-dimensional Interpolation Scheme for Computational Aeroacoustics Applications Using Overset Grid, AIAA paper 2004-2812, 2004.
- [26] C.K.W. Tam, J.C. Webb, Dispersion-relation-preserving finite difference schemes for computational acoustics, J. Comput. Phys. 107 (1993) 262–281.
- [27] K. Taylor, A transformation of the acoustic equation with implications for wind-tunnel and low-speed tests, Proc. R. Soc. Lond. A. 363 (1978) 271–281.
- [28] A. Tinetti, M. Dunn, Aeroacoustic Noise Prediction Using the Fast Scattering Code, AIAA paper 2005-3061, 2005.